Biological Implication of Conformational Flexibility in Ouabain: Observations with Two Ouabain Phosphate Isomers†

Akira Kawamura,‡,§ Leif M. Abrell,‡ Federica Maggiali,‡ Nina Berova,‡ Koji Nakanishi,*,‡ Jason Labutti,|| Sheila Magil,|| Garner T. Haupert, Jr.,⊥ and John M. Hamlyn*,#

Department of Chemistry, Columbia University, New York, New York 10027, BION Inc., 840 Memorial Drive, Riverside Technology Center, Cambridge, Massachusetts 02139, Renal Unit, Medical Services, Massachusetts General Hospital, Harvard Medical School, Charlestown, Massachusetts 02129, and Department of Physiology, University of Maryland at Baltimore, Baltimore, Maryland 21201

Received January 26, 2001; Revised Manuscript Received March 14, 2001

ABSTRACT: Ouabain is a highly polar and unusually potent sodium pump inhibitor that possesses uncommon conformational flexibility in its steroid A-ring moiety. The biological significance of ring flection in the cardiotonic steroids has not been described. Accordingly, we prepared ouabain 1,5,19- and 1,11,19-phosphates. The former stabilizes the steroid A-ring chair conformation and the latter locks the A-ring in the half-boat conformation and decreases flection of the ABC-ring moiety. Using a dog kidney cell line (MDCK) in a pH microphysiometer (Cytosensor), ouabain and its 1,5,19-phosphate at 10^{-5} M reduced the rate of extracellular acidification by 15−20%. During inhibitor washout, the rate of recovery from the 1,5,19-phosphate analogue was ∼3 times faster than ouabain. The 1,11,19-phosphate at 10^{-4} M elicited a weak (∼7%) response, and the effects reversed ∼44-fold faster than ouabain. Studies with purified Na^+,K^+-ATPase showed that ouabain and its 1,5,19-phosphate analogue were of similar efficacy (EC_{50} = 1.1 and 5.2 × 10^{-7} M, respectively) and >100-fold more potent than the 1,11,19-phosphate analogue. Studies of the binding kinetics showed that the 1,5,19-phosphate analogue bound 3-fold and dissociated 16-fold faster from the purified Na^+,K^+-ATPase than ouabain. Both analogues were competitive inhibitors of ^{3}H-ouabain binding. Taken together, these results suggest that the marked conformational flexibility of the A-ring in ouabain ordinarily slows the initial binding of this steroid to the sodium pump. However, once ouabain is bound, flection of the steroidal A- and BC-rings is critical for the maintenance of high-affinity binding. Our results indicate that the ouabain-binding site is comprised of structurally mobile elements and highlight the roles that synchronization between receptor and ligand dynamics play as determinants of biological activity in this system.

Among the most potent cardiotonic steroids (cardenolides/digitalis toxins), ouabain (**1**, Figure 1) has been widely used in biomedical research as a specific inhibitor of the sodium pump. Ouabain preferentially stabilizes a phosphorylated intermediate (E_2P) in the reaction cycle of the sodium pump and thereby stops ATP hydrolysis and active Na^+, K^+ transport across the plasma membrane (*5*). Ouabain has long been known to originate in certain plants. However, recent observations, including possible biosynthesis in cultured adrenocortical cells (*1*, *9*) as well as numerous findings of ouabain-like steroids in various mammalian tissues (*3*, *4*, *6*, *9*, *17*), suggest that its endogenous counterpart has an important physiological role in mammals (*4*).

A series of pioneering observations by Yoda and co-workers raised the possibility of dynamic conformational changes of the cardenolide binding site of the sodium pump during the association and dissociation of cardiac glycosides (*24*). During the association of cardiac glycosides with the sodium pump, it is believed that the aglycon moiety binds first and that this event subsequently opens a binding pocket for the sugar moiety. This view is supported by the fact that rhamnose does not inhibit ouabain binding whereas cardenolide genins do (*22*, *24*). The dissociation of ouabain, on the other hand, is thought to begin with dissociation of the sugar moiety, followed by a conformational change that closes the sugar binding site and facilitates unbinding of the aglycon moiety (*23*). Prior studies of structure−activity relationships (SAR) among the cardiac glycosides showed that the conserved cardenolide C/D-ring cis structure confers specificity for the sodium pump (*19*, *21*). Therefore, the initial phase of ouabain binding is most likely mediated through the D-ring and lactone moieties. Subsequent slow binding of rhamnose then anchors the ouabain molecule tightly to the sodium pump, as revealed by its ∼80-fold slower dissociation rate than ouabagenin (*25*).

While the lactone, D-ring, and rhamnose moieties of ouabain are important for biological activity and potency as

†This work was supported by Grants HL52282 (G.T.H./K.N.) and AI10187 (K.N.) from the National Institutes of Health, by a National Institutes of Health National Research Service Award (L.M.A.), and in part by the American Heart Association and NIDDK 53492 (J.M.H.).

* Corresponding authors. K.N.: e-mail, kn5@columbia.edu; telephone, 212 854 2169; fax, 212 932 8273. J.M.H.: e-mail, jhamlyn@umaryland.edu; telephone, 410 706 3479; fax, 410 706 8341.

‡ Department of Chemistry, Columbia University in the City of New York.

§ Current address: The Scripps Research Institute, La Jolla, CA.

|| BION Inc., Cambridge, MA.

⊥ Massachusetts General Hospital, Harvard Medical School, MA.

Department of Physiology, University of Maryland.

10.1021/bi0101751 CCC: $20.00
Published on Web 04/18/2001

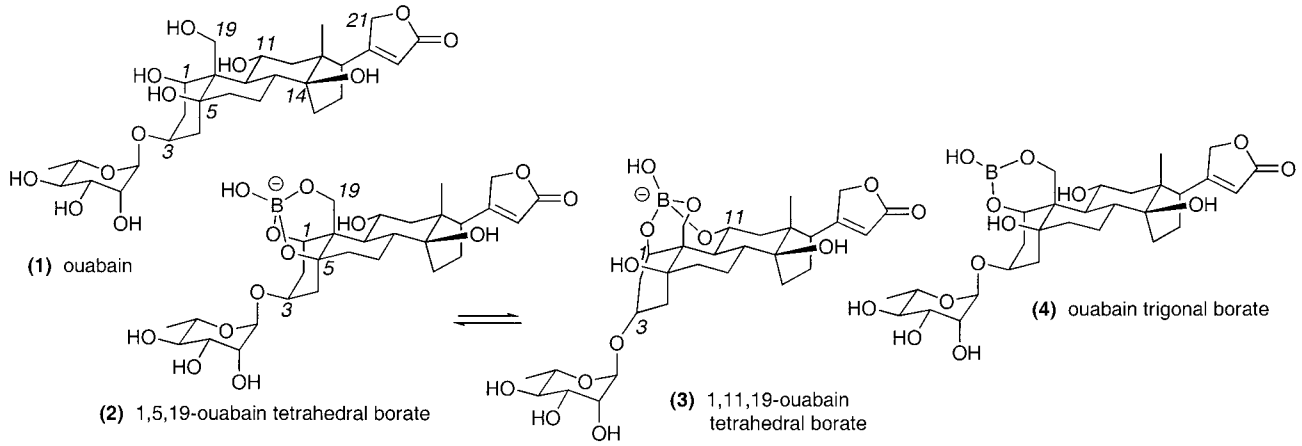

FIGURE 1: Structure of ouabain and ouabain borates. Two interconverting tetrahedral coordination isomers of ouabain borate exist as **2** and **3**. The major isomer has an A-ring boatlike conformation, whereas the A-ring in the minor isomer is in the chair form. A ouabain trigonal borate (**4**) also exists.

described above, it is not clear whether the structure of the A/B/C ring region influences the biological activity of ouabain. Previous NMR[1] based studies on ouabain by us (*6*) and others (*13*, *17*) showed that the A-ring moiety possesses unexpectedly high conformational flexibility. Ouabain probably has a smaller energy difference between the A-ring chair and twist-boat conformations than other cardenolides due to the combination of an A/B-cis-ring fusion and a 1,3,5-triaxial substitution pattern with rhamnose at the 3-position. The presence of the rhamnose appears to have a large effect on the conformational profile of the A-ring because the ^{1}H NMR of ouabain shows a broadened 1-H signal, whereas the 1-H resonance of ouabagenin is much sharper under the same conditions (D_2O, room temperature). While both ouabain and ouabagenin have multiple A-ring conformers as shown by low-temperature NMR measurements (*13*), the 1-H signal profile at room temperature indicates that the A-ring conformational exchange in ouabain is slower than that of ouabagenin. The A-ring flexibility becomes evident when ouabain forms the labile borate complexes 1,5,19-tetrahedral borate (**2**) and 1,11,19-tetrahedral borate (**3**) in which the latter is a ring-A boatlike conformer and is more abundant (Figure 1). Under certain conditions, ouabain also forms a trigonal borate (**4**) with an undetermined borate linking site (*6*). This conformational flexibility may be biologically important since it can affect the distance between the lactone on the D-ring and the rhamnose moiety. The distance between 21-C and 3-O in the A-ring boatlike conformer is approximately 10.4 Å, i.e., ~0.4 Å longer than that of the chair conformer (*7*). This seemingly small structural change may allow ouabain to interact more effectively with those parts of its binding site that are affected by conformational changes during the catalytic cycle of the sodium pump.

To examine the biological significance of A-ring flexation, two novel and stable conformationally locked ouabain analogues were prepared, and their interaction with the sodium pump was evaluated with a cell-based pH microphysiometer (Cytosensor, Molecular Devices Corp., Sunnyvale, CA) (*15*) as well as with binding kinetic analyses using purified Na^+,K^+-ATPase. The two conformationally locked analogues of ouabain, i.e., the 1,5,19- and 1,11,19-phosphate isomers, were prepared by a single step phosphorylation of ouabain with phosphorus oxychloride and represent the A-ring chair and half-boat conformations, respectively.

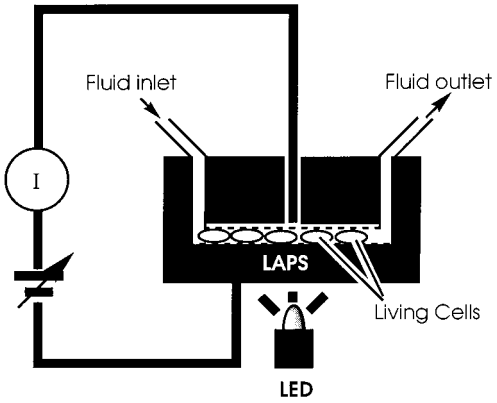

FIGURE 2: Cytosensor (microphysiometer). The extracellular acidification rate is monitored by a silicon-based light-addressable potentiometric sensor (LAPS). Since cellular ATP hydrolysis is tightly coupled to ATP synthesis by oxidative metabolism (respiration) and glycolysis, sodium pump inhibition results in reduction of the extracellular acidification rate.

We used a Cytosensor (pH microphysiometer) instrument to detect cellular metabolic activity by monitoring the rate at which cells excrete acidic metabolites (i.e., lactic acid, CO_2) into the extracellular environment (*15*) (Figure 2). The Madin−Darby canine kidney (MDCK) cell line was used because the α-1 isoform of the sodium pump accounts for a large fraction of cellular metabolic activity in this preparation (*2*, *11*, *12*). Accordingly, inhibition of the sodium pumps on MDCK cells leads to a large reduction in the rate of extracellular acidification. Using the Cytosensor, we recorded the rates of extracellular acidification every 2 min for a period of several hours to provide a near real time long time measurement of sodium pump activity in living cells. During this several hour assay period, ouabain, its 1,5,19- and 1,-11,19-phosphate analogues, and ouabagenin were applied to the cells and then washed away to examine real time cellular metabolic responses mediated by the sodium pump. In addition, the binding kinetics of the inhibitors were examined

[1] Abbreviations: MDCK, Madin−Darby canine kidney; DMEM, Dulbecco's modified Eagle medium; FBS, fetal bovine serum; SAR, structure−activity relationship; MS, mass spectrometry; NMR, nuclear magnetic resonance; ROESY, rotating-frame nuclear Overhauser effect spectroscopy; LAPS, light-addressable potentiometric sensor; LED, light-emitting diode.

using a purified dog kidney Na^+,K^+-ATPase in a coupled optical assay. On the basis of the data from the cell- and enzyme-based assays, unexpectedly large effects of A-ring flection on the biological potency of ouabain have been discerned.

MATERIALS AND METHODS

Materials. Ouabain octahydrate was from ACROS (Fair Lawn, NJ), and ^{3}H-ouabain was from Amersham Pharmacia Biotech, Inc. (Piscataway, NJ). All other chemicals and HPLC solvents were from Aldrich (Milwaukee, WI). MDCK cells were obtained from ATCC (Manassas, VA). Penicillin−streptomycin, Fungizone, 2.5% trypsin, Hanks' balanced salt solution (HBSS) without Ca^{2+} and Mg^{2+}, and Dulbecco's modified Eagle medium (DMEM) were from Gibco BRL (Rockville, MD). Fetal bovine serum (FBS) (BioWhittaker, Walkersville, MD), culture flasks, pipets, and vials were from Fisher (Suwanee, GA). The extracellular acidification rate was measured with Cytosensor (Molecular Devices, Sunnyvale, CA), and data were processed with Cytosoft Version 2.0.1. Na^+,K^+-ATPase was obtained partially purified from the outer medulla of dog kidney (Sigma, St. Louis, MO). NMR spectra were recorded on a Bruker DMX500 (^{1}H, COSY, HMQC, HMBC, ROESY, and NOESY) or a Bruker DRX300WB (^{13}C, DEPT, ^{31}P) spectrometer. For ouabain 1,5,19-phosphate, 50% acetonitrile-d_3 in deuterium oxide was used for the NMR solvent, whereas methanol-d_4 was used for ouabain 1,11,19-phosphate. The methyl group of acetonitrile-d_3 or methanol-d_4 was used as an internal standard for the ^{1}H and ^{13}C NMR chemical shifts. H_3PO_4 (85%) was used as an external standard for the chemical shift of ^{31}P NMR. Electrospray mass spectrometry was performed with a Micromass Q-TOF instrument (Manchester, U.K.).

Preparation of Conformationally Locked Ouabain Analogues. Water in ouabain octahydrate (500 mg, 0.69 mmol) was azeotropically removed with anhydrous pyridine (50 °C; repeated three times), and the resulting material was dried in vacuo. The dried ouabain was dissolved in a mixture of pyridine/CH_2Cl_2/THF (tetrahydrofuran)/DMF (0.5, 10, 15, and 2.5 mL, respectively), stirred at ambient temperature for 10 min in the presence of molecular sieves, 4 Å (powder), and cooled to −78 °C. To this solution was added phosphorus oxychloride [10% (v/v) in THF, 2.5 mL, 2 equiv] dropwise over a 15 min period. The solution turned into a white suspension while it was being stirred at −78 °C for 1 h. The reaction mixture was poured into ice−water containing 5% $NaHCO_3$ (w/v), extracted to water, evaporated at 50 °C to remove residual volatile solvents, and filtered. The resulting crude aqueous solution was dried at 80 °C in vacuo. The dried material was purified with silica gel column chromatography (20% MeOH in $CHCl_3$). A mixture of ouabain 1,5,19- and 1,11,19-phosphates, which appeared as a single spot on TLC (R_f 0.35, 40% MeOH in $CHCl_3$), was collected and concentrated (168 mg; 40% yield as a mixture). A large amount of ouabain (287 mg) was recovered from the reaction.

The mixture of 1,5,19- and 1,11,19-phosphates was further purified with RP-HPLC (Waters NovaPak HR C_{18}, 7.8 × 300 mm, 60 Å, 6 μm; a linear gradient of 0−25% acetonitrile in water over 15 min, followed by a 25−50% acetonitrile gradient over 5 min; 3 mL/min; UV 220 nm). For biological studies, purification was repeated to obtain a single peak for each sample. The NMR spectroscopic data of the two compounds are summarized in Table 1.

Table 1: ^{1}H, ^{31}P, and ^{13}C NMR of Ouabain 1,5,19- and 1,11,19-Phosphates

ouabain 1,5,19-phosphate acetonitrile-d_3/D_2O (1:1) (310 K) ^{31}P NMR[a] (δ) −6.63 ppm (m)			ouabain 1,11,19-phosphate MeOH-d_4 (300 K) ^{31}P NMR[a] (δ) −7.34 ppm (m)	
^{13}C	^{1}H	no.	^{13}C	^{1}H
86.5	5.88	1	85.3	4.35
32.1	2.28 (2H)	2	38.3[c]	2.45, 1.94
71.0	4.09	3	70.7	3.70
34.8	2.35, 2.03	4	44.5[c]	1.96, 1.78
89.7		5	74.1	
32.5	2.07, 1.68	6	32.2[c]	1.71, 1.55
24.0	2.04, 1.29	7	22.3	2.10, 1.59
39.7	1.69	8	36.9[c]	2.54
46.0	1.72	9	52.3	2.05
42.0		10	46.3	
67.2	3.60	11	75.8[c]	4.59
49.4	1.65, 1.40	12	46.0	1.98, 1.72
50.6		13	50.8	
85.1		14	86.1	
34.8	2.11, 1.82	15	33.6	2.20, 1.84
27.4	2.09, 1.77	16	27.4	2.21, 1.88
50.5	2.82	17	51.7	2.96
17.0	0.85	18	16.9	1.01
73.4	5.11, 4.68	19	71.0	4.82 (2H)
177.8[b]		20	177.0[b]	
75.3	4.90	21	75.3	4.98
117.6	5.85	22	118.5	5.95
177.6[b]		23	177.1[b]	
99.9	4.77	1′	100.5	4.83
71.8	3.76	2′	72.6	3.76
71.4	3.65	3′	72.4	3.64
73.1	3.33	4′	74.0	3.37
69.6	3.72	5′	70.3	3.65
17.7	1.20	6′	18.0	1.26

[a] ^{31}P NMR external reference is 85% H_3PO_4. [b] Assignments in the same column may be reversed. [c] Signal broadening observed.

Culture of MDCK Cells. MDCK cells were cultured in DMEM containing 10% FBS, 50 units/mL penicillin, 50 μg/mL streptomycin, and 125 ng/mL Fungizone in a humidified, 37 °C, 5% CO_2 incubator. Cells were subcultured at 70−90% confluency.

Microphysiometry Assay. The assay was carried out by following the standard protocol provided by the manufacturer (Molecular Devices, Sunnyvale, CA). Briefly, MDCK cells were plated into the Cytosensor capsule cups (1×10^5 cells/cup) 1 day prior to the experiment and placed in a humidified 5% CO_2 incubator at 37 °C overnight. The assay medium was prepared from powdered DMEM without sodium bicarbonate, to which NaCl was added to balance the osmotic pressure (final 130 mM). The assay medium was adjusted to pH 7.2 by NaOH, supplemented with 1% FBS, 100 units/mL penicillin, and 100 μg/mL streptomycin, and sterile filtered. The addition of 1% FBS in the assay medium was necessary to obtain a stable cellular acidification rate from MDCK cells because the acidification rate drifts down in serum-free media. Measurements were carried out using a 2 min pump cycle protocol. In this protocol, the cells were perfused with the assay medium for 80 s at approximately 100 μL/min (50% perfusion pump power), followed by measurement of the acidification rate with the perfusion pump off during the remaining 40 s. After the acidification rate reached a stable baseline level (∼1 h), media containing

Scheme 1: Preparation of Conformationally Locked Ouabain Analogues

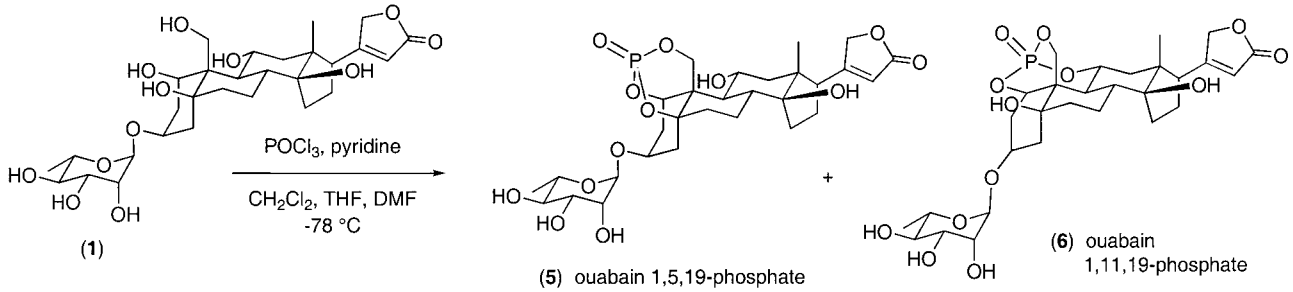

the indicted inhibitors were applied to the cells for a period of 6 min (i.e., three perfusion pump cycles) and then washed out from the cell chamber. The effects of inhibitors were visualized by inspection of the acidification rates before, during, and after treatment (recovery). Acidification rate experiments were performed at least six times for each sample (except ouabagenin, two times), and the depicted data are representative of several trials.

Dog Kidney Na^+,K^+-ATPase Assay. Partially purified dog kidney Na^+,K^+-ATPase was suspended typically at ~1.5 mg/mL in 10 mM TES-tris [*N*-[tris(hydroxymethyl)methyl]-2-aminoethanesulfonic acid] (pH 7.4) containing 1 mM each of EGTA and EDTA. Assays were initiated typically by addition of 10 μL aliquots of enzyme to the ATP-regenerating system with and without the inhibitors of interest. Measurements of enzyme activity were made at 37 °C in 1 mL of an ATP-regenerating cocktail whose activity was followed optically (*18*) by the oxidation of NADH (ϵ 6220, 340 nm). The final assay mixture contained 20 mM KCl, 100 mM NaCl, 6 mM Mg_2SO_4, 5 mM EGTA, 3 mM ATP-Na_2, 2 mM phosphoenolpyruvate−monocylohexylammonium, 0.3 mM NADH, 100 mM TES-tris, pH 7.4, 11 units of LDH, and 12 units of pyruvate kinase. ATPase activity was determined continuously by following the decrease in absorbance at 340 nm using a Beckman Du8b spectrophotometer in the rate mode. Under optimal conditions, ~98% of the total ATPase activity (measured specific activity ~4 μmol min^{-1} mg^{-1}) was inhibited by 10^{-5} M ouabain. The maximal capacity of the regenerating system was >4000 times more than the maximal ATPase activity. In experiments where the dissociation rates were desired, the inhibitors were preincubated for 15 min at 37 °C with the ATPase in a potassium-free coupled assay mixture (total volume 50 μL). Subsequently, 10 μL aliquots were diluted 100-fold into the normal regenerating assay. In some experiments where long recordings were desired, the amount of ATPase used was reduced to avoid exhaustion of NADH. The Na,K-ATPase experiments were performed in triplicate in three experiments. The data presented are the mean values and are representative of the separate trials. The experimental standard errors were typically <7%.

^{3}H-Ouabain Binding Studies. Binding of ^{3}H-ouabain (Amersham) was performed in 0.67 mL of a medium containing 0.5 mM EDTA, 5 mM $MgCl_2$, 5 mM Na_2HPO_4, and 10 mM TES-tris, pH 7.4. For Scatchard analysis, the [^{3}H-ouabain] was varied from 1 to 50 nM. In parallel reactions, ouabain 1,5,19-phosphate (25 nM) or ouabain 1,11,19-phosphate (500 nM) was included. In each case, binding was initiated by addition of dog kidney Na^+,K^+-ATPase, and the reaction was run for 3 h at 37 °C. The reaction was quenched by addition of 2 mL of ice-cold binding medium containing 100 μM unlabeled ouabain. Nonspecific binding was estimated by inclusion of 100 μM unlabeled ouabain. Bound ^{3}H was trapped by vacuum filtration over glass fiber filters (Whatman GF/B). The filters were soaked in scintillation solution (RPI Biosafe II) for 12 h, and ^{3}H was determined by scintillation counting and corrected for quench. Specific binding was obtained by subtraction of nonspecific from total counts bound. Binding experiments were performed in quadruplicate, and the data shown are representative of two separate experiments. The data shown are mean values and representative of the trials. The experimental standard errors were typically <3%.

RESULTS

Preparation of Conformationally Locked Ouabain Analogues. Ouabain 1,5,19- and 1,11,19-phosphates (**5** and **6**, respectively) were prepared by a treatment of ouabain in pyridine-containing solvent with phosphorus oxychloride at −78 °C (Scheme 1). A mixture of the two phosphates (40% yield as a mixture) was obtained after silica gel chromatography. Each isomer was then purified by repetitive RP-HPLC.

Structures of the two isomeric phosphates were characterized by MS and NMR. Electrospray MS of ouabain 1,5,19-phosphate gave signals at *m/z* 650.7 $(M + Na)^+$, and 666.7 $(M + K)^+$, whereas signals at *m/z* 628.7 $(M)^+$, 650.8 $(M + Na)^+$, and 666.8 $(M + K)^+$, corresponding to a molecular formula of $C_{29}H_{41}O_{13}P$, were obtained for the 1,11,19-phosphate. The difference between the molecular mass of 628 and ouabain (MW 584) corresponds to the addition of a single P═O group (+47) and removal of three H's (−3), indicating that the phosphate group in each isomer was attached to three hydroxyl groups on the ouabain molecule. ^{13}C NMR of ouabain 1,5,19-phosphate showed two bond P−C couplings ($^2J_{PC}$) at 1-C (86.5 ppm, $J = 5.7$ Hz), 5-C (89.7 ppm, $J = 4.6$ Hz), and 19-C (73.4 ppm, $J = 4.6$ Hz) signals, which confirmed the phosphorylation site. The A-ring of the 1,5,19-phosphate is, therefore, locked in the chair conformation. ^{13}C NMR of 1,11,19-phosphate gave clear $^2J_{PC}$ couplings at 1-C (85.3 ppm, $J = 5.7$ Hz) and 19-C (71.0 ppm, $J = 7.0$ Hz). Coupling between phosphate and 11-C was obscured by ^{13}C signal broadening, but a three bond P−C coupling, $^3J_{PC}$, between the phosphate group and 12-C confirmed the phosphate attachment site. A ROESY cross-peak between 1-H and 9-H of the 1,11,19-phosphate (data not shown), which was also observed for ouabain 1,11,19-borate (**3**) (*6*), supported the A-ring half-boat conformation.

Microphysiometer Assay. Ouabain and its 1,5,19- and 1,11,19-phosphate analogues were examined by pH micro-

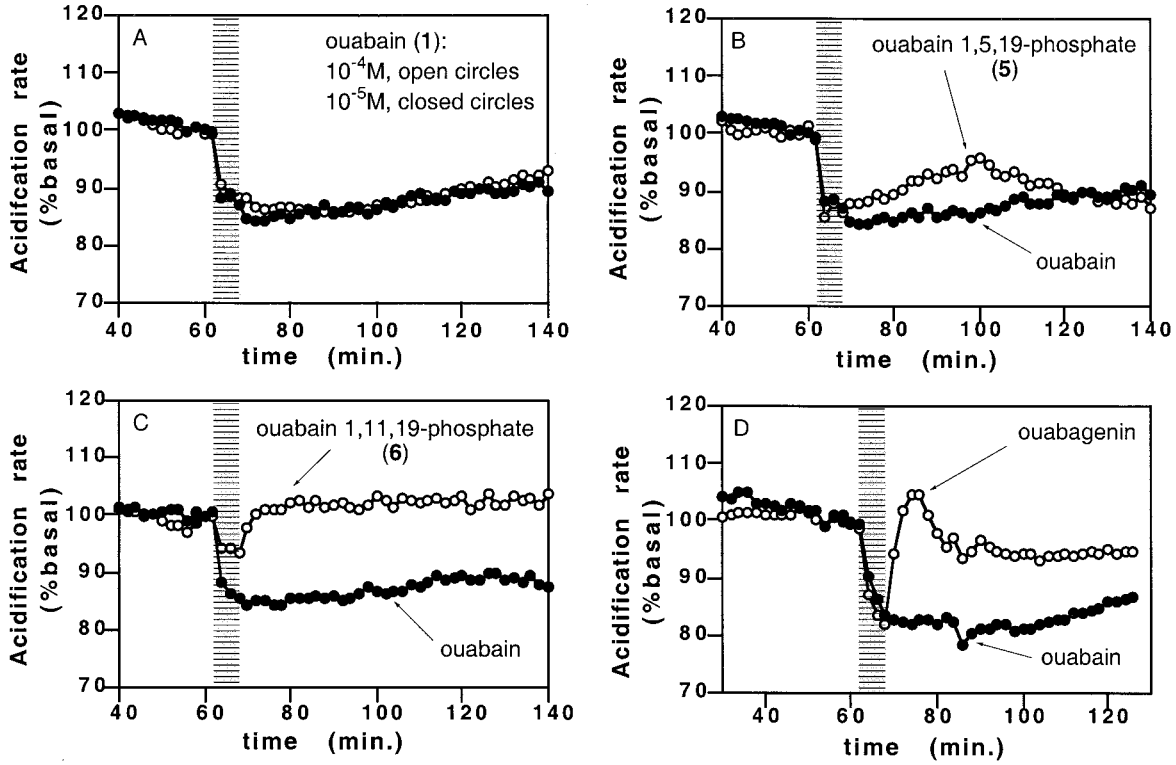

FIGURE 3: Treatment of MDCK cells with sodium pump inhibitors: (A) ouabain at 10^{-4} M (○) and 10^{-5} M (●); (B) ouabain 1,5,19-phosphate (○) and ouabain control (●) at 10^{-5} M; (C) ouabain 1,11,19-phosphate (○) and ouabain control (●) at 10^{-4} M; (D) ouabagenin (○) and ouabain control (●) at 10^{-5} M. MDCK cells were perfused with a running medium (DMEM), and acidification rates were obtained every 2 min. After a stable acidification rate was reached, cells were perfused with a sample containing medium for a period of 6 min (hashed area) before being perfused again with the running medium.

physiometry using MDCK cells (Figure 3). Accumulation of extracellular acid was monitored by a silicon-based light-addressable potentiometric sensor (LAPS) coupled with a light-emitting diode (LED) (*15*). Inhibition of the sodium pump results in a decrease in the amount of cellular ATP hydrolysis, which in turn suppresses both oxidative phosphorylation (respiration) and glycolysis because of the tight coupling between ATP hydrolysis and synthesis in MDCK cells (*11*, *12*). Inhibition of the sodium pump reduces the production of CO_2 and lactic acid and decreases the rate of extracellular acidification. In response to the inhibitors, the kinetics of the pH response provide indirect qualitative measures of inhibitory potency and the dissociation profile.

Ouabain was examined with the Cytosensor to establish the assay conditions. Application of media containing 10^{-5} and 10^{-4} M ouabain to MDCK cells for 6 min lowered the rate of cellular acidification to ~80−85% of the original (pretreatment) level in both cases (Figure 3A). The nearly equal responses to the two concentrations indicate that sodium pumps on the MDCK cells were essentially saturated with 10^{-5} M ouabain under our assay conditions. Suppression of the acidification rate persisted even after withdrawal of ouabain from the medium. This is in accordance with the well-known tight binding (slow "off-rate") profile of ouabain to the sodium pump (*20*, *24*, *25*). By using the recovery profile of the acidification rate, the first order "recovery rate constant" was estimated to be about 7.7×10^{-3} min^{-1}. Since ouabain concentrations below 10^{-5} M gave less consistent cell responses (data not shown), a saturating concentration (10^{-5} or 10^{-4} M) was used as a positive control for subsequent cell experiments.

The conformationally locked ouabain analogues were then examined with the Cytosensor. When 10^{-5} M ouabain 1,5,-19-phosphate (**5**, A-ring chair) was added to the MDCK cells, a clear decrease in the acidification rate was observed (Figure 3B), and the effect was comparable to that observed with ouabain at the same concentration. Following washout of the analogue, the acidification rate recovered with a rate constant of ~2.3×10^{-2} min^{-1}, i.e., ca. 3-fold faster than with ouabain. Therefore, the A-ring chair-locked analogue appeared to retain the potency of ouabain but dissociated somewhat more rapidly than ouabain. The 1,11,19-phosphate (**6**), on the other hand, exhibited a totally different profile from ouabain and its 1,5,19-phosphate analogue. The compound had little or no detectable inhibitory activity at 10^{-5} M (not shown). At 10^{-4} M this A-ring half-boat analogue caused 7−8% suppression of the acidification rate (Figure 3C). When the analogue was washed out, the acidification rate returned to the basal level rapidly (rate constant ~0.34 min^{-1}), i.e., ~44 times faster than ouabain in this assay system. Finally, the readily reversible inhibitor ouabagenin (=ouabain 3-OH) at 10^{-5} M suppressed the rate of acidification (Figure 3D) to an extent comparable to that of ouabain. Upon washout of ouabagenin, the cells recovered rapidly as expected from its fast rate of dissociation from the sodium pump (*25*). Often an "overshoot" of the rate of acidification was observed which then slowly fell back to the basal level. The recovery rate constant of ouabagenin was, therefore, difficult to estimate, although it was apparently of a magnitude similar to that of ouabain 1,11,19-phosphate.

Dog Kidney Na^+,K^+-ATPase Assay. We used a coupled optical assay to measure the activity of the isolated Na^+,K^+-

Table 2: Summary of Rate Constants from the Na^+,K^+-ATPase Assay

	k_{on}(app) (min^{-1})	k_{off} (min^{-1})	k_{on}(corr) (min^{-1} mol^{-1})	K_{diss} (M)
ouabain (**1**)	0.414 at 10^{-6} M	0.0188	4.33×10^5	4.15×10^{-8}
ouabain 1,5,19-phosphate (**5**)	1.2 at 10^{-6} M	0.299	1.49×10^6	1.99×10^{-7}
ouabain 1,11,19-phosphate (**6**)	0.437 at 10^{-4} M	fast (~5)	$\sim 5.44 \times 10^4$	$\sim 9.19 \times 10^{-5}$

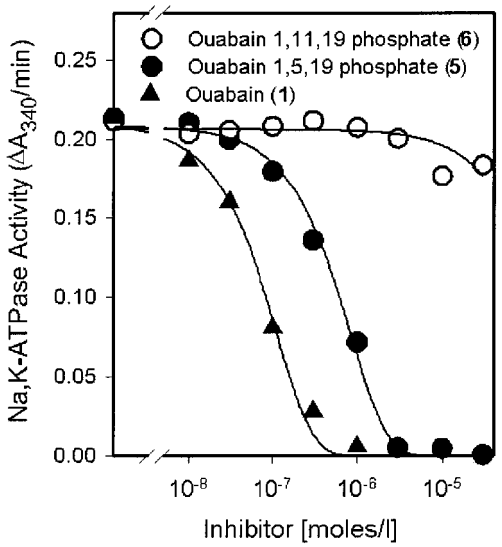

FIGURE 4: Dose−response relationships for inhibition of dog kidney Na^+,K^+-ATPase by ouabain and ouabain 1,5,19- and 1,11,19-phosphates. The reaction was started by addition of 10 μL of Na^+,K^+-ATPase (15 μg) to 990 μL of the ATP-regenerating cocktail (37 °C, see Materials and Methods) that contained the inhibitors at the final concentrations shown. Final assay concentrations of the primary ligands were 20 mM K^+, 100 mM Na^+, 6 mM Mg^{2+}, and 3 mM ATP. Computations of the rate of oxidation of NADH were made at 30-s intervals. The relationships shown were derived from rate measurements taken 12 min after the start of the reaction. The data were fitted by iterative nonlinear regression to the equation: ATPase activity = maximal activity/$(1 + [\text{inhibitor}]/EC_{50})^n$.

ATPase. In this system, the hydrolysis of ATP to ADP by the Na^+,K^+-ATPase is coupled to the oxidation of NADH by an ATP-regenerating system including pyruvate kinase, lactate dehydrogenase, and phosphoenolpyruvate. None of the ouabain/analogue inhibitors interfered with the coupled enzymes as judged by the rates of NADH oxidation in response to addition of ADP (not shown).

Figure 4, shows the striking difference in the inhibitory potencies of the two phosphorylated isomers **5** and **6**. The dose-inhibition curve for **5** was well fit ($r > 0.98$) by the equation of a single site model and yielded a Hill coefficient of 0.97. Comparisons of the EC_{50} values for ouabain (**1**, 1.1×10^{-7} M) and ouabain 1,5,19-phosphate (**5**, 5.3×10^{-7} M) under these reaction conditions confirmed that **5** retained much of the inhibitory potency of ouabain. In contrast, the 1,11,19-phosphate (**6**) was devoid of significant inhibitory activity at concentrations up to 10^{-5} M (Table 2). In other experiments, partial inhibition (~40%) of ATPase activity by ouabain 1,11,19-phosphate at 10^{-4} M was detected (not shown). The experimental design and solubility concerns prevented us from using higher concentrations of the 1,11,19 analogue.

Detailed analyses of the kinetics of the interactions of these inhibitors with Na^+,K^+-ATPase were revealing. The experiments were performed in two ways. For association studies, the ATPase reaction was started and allowed to run at steady state for 3−6 min as indicated. Then, small aliquots of inhibitors were added to achieve the indicated concentrations, and semicontinuous recordings were made of the decline in Na^+,K^+-ATPase activity until evidence of a new steady state was apparent. For dissociation studies, the inhibitors were allowed to bind to the ATPase under type I phosphorylating conditions (i.e., Mg^{2+} + ATP + Na^+) in the absence of potassium. Then, aliquots were diluted 100-fold into the final assay so that the new concentration of inhibitors would be too low to cause significant inhibition. Under these conditions, the dissociation kinetics of the inhibitors could be ascertained from the recovery of ATPase activity. In addition, the presence of physiological concentrations of potassium in the final assay would further minimize any tendency to rebind free inhibitor.

The kinetics of inhibition by ouabain (**1**) and its 1,5,19-phosphate analogue (**5**) both at 10^{-6} M are shown in Figure 5A. The 1,5,19-analogue inhibited the ATPase more rapidly than ouabain, eventually reaching a lower steady-state level of inhibition as expected from the dose−response comparisons. In each case, the data were fit well by a monoexponential decay function and yielded apparent rate constants of 0.414 and 1.2 min^{-1} for ouabain and the analogue, respectively.

Figure 5B shows the dissociation kinetics for the unbinding of ouabain and the 1,5,19-phosphate analogue to the ATPase. Each inhibitor (10^{-6} M) was allowed to reach equilibrium binding with the enzyme. Following dilution of the preformed ouabain−enzyme complexes into the nominally inhibitor-free coupled assay, the Na^+,K^+-ATPase activity rose slowly with a monoexponential rate constant of 0.0188 min^{-1}. Under identical conditions the activity of the ouabain 1,5,19-phosphate treated enzyme returned to control within 15 min with kinetics that were well described by a single exponential rate constant of 0.299 min^{-1}. Thus, the 1,5,19-phosphate (A-ring chair) dissociated ~16 times faster from the dog kidney enzyme than ouabain. As shown in Table 2, the apparent association rate constant for the binding of this analogue with the enzyme was ~3-fold faster than with ouabain. Therefore, the overall binding interaction of the 1,5,19-phosphate analogue with the ATPase was ~5-fold weaker than with ouabain, consistent with the data in Figure 4.

The kinetics of the inhibition of the Na^+,K^+-ATPase by the 1,11,19-phosphate (**6**, A-ring half-boat) (Figure 6) implied that this analogue bound slowly. The calculated rate (0.44 min^{-1} at 10^{-4} M, Table 2) was approximately 2 orders of magnitude slower than ouabain (**1**) or the 1,5,19-phosphate (**5**). Efforts to measure the dissociation rate constant for this analogue were not successful because of its rapidity. For example, following a preincubation with 10^{-4} M 1,11,19-phosphate (**6**), ~40% of the ATPase activity was inhibited, but within the first 15 s of dilution of the ATP-regenerating assay mixture, the ATPase activity was near normal. Therefore, a specific value for k_{off} could not be obtained with

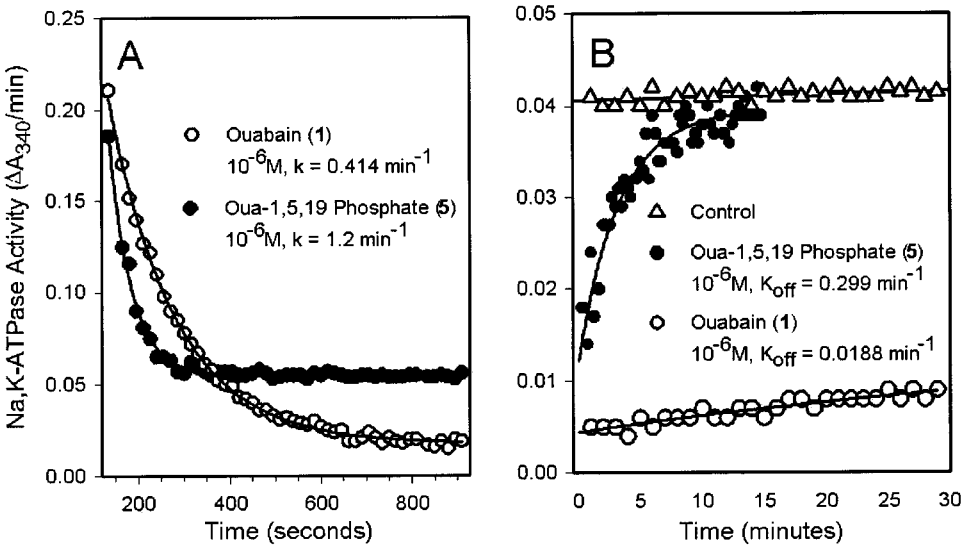

FIGURE 5: Kinetics of the interaction of ouabain 1,5,19-phosphate and ouabain with Na^+,K^+-ATPase. (A, left panel) Kinetics of inhibition of the dog kidney Na^+,K^+-ATPase by ouabain 1,5,19-phosphate and ouabain. The reaction was started by addition of 10 μL of Na^+,K^+-ATPase (15 μg) to 890 μL of the ATP-regenerating cocktail (37 °C, see Materials and Methods). After ~3 min, when ATPase activity was at steady state, 100 μL aliquots of prewarmed inhibitor solution were added to attain final concentrations of 10^{-6} M. Automatic computations of the rate of oxidation of NADH were made at 15-s intervals. Final conditions of the primary ligands were 5 mM K^+, 100 mM Na^+, 6 mM Mg^{2+}, and 3 mM ATP. The solid lines were fitted by iterative nonlinear regression to an equation describing first-order exponential decay. Derived values for the apparent first-order rate constant for binding [k_{on}(app)] are shown in Table 2. (B, right panel) Kinetics of Na^+,K^+-ATPase activity during dissociation of ouabain 1,5,19-phosphate and ouabain. 20 μL aliquots of Na^+,K^+-ATPase were mixed with 20 μL of potassium-free ATP-regenerating cocktail and either 10 μL of water (control) or inhibitors at 10^{-6} M (ouabain, ○; ouabain 1,5,19-phosphate, ●) final concentrations. Following preincubation for 15 min at 37 °C, 10 μL aliquots were introduced into 990 μL of the ATP-regenerating cocktail, and the rates of NADH oxidation were followed for periods up to 30 min. Rate computations for ATPase derived from the control and ouabain preincubations were made at 1-min intervals. Rate calculations were performed at 15-s intervals for the ouabain 1,5,19-phosphate preincubated enzyme. The solid lines were fitted to the data by iterative nonlinear regression to an equation [$Y = Y_0 + a(1 - e^{-bx})$] describing first-order exponential association.

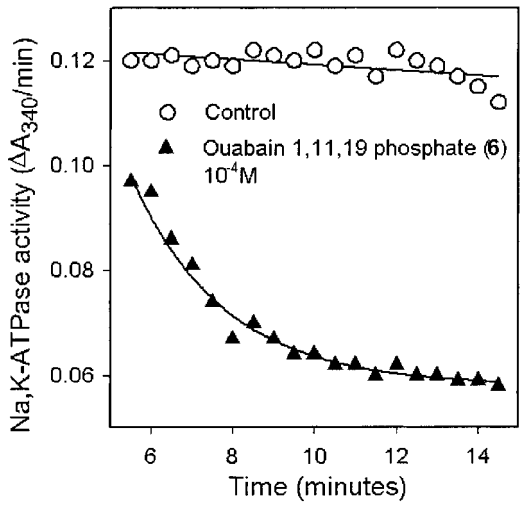

FIGURE 6: Kinetics of the interaction of ouabain 1,11,19-phosphate and Na^+,K^+-ATPase. The reaction was performed essentially as described in the left panel of Figure 5. The solid lines were fitted by iterative nonlinear regression to an equation describing first-order exponential decay. Derived values for the apparent first-order rate constant for binding [K_{on}(app)] are shown in Table 2. The solid lines were fitted to the data as described in the legend of Figure 5.

our facilities, although it is likely that it was >5 min^{-1}. When correction of the apparent rate constant for the binding (Table 2) of the 1,11,19-phosphate was made using the estimated dissociation rate, the binding of the 1,11,19-phosphate was found to be ~12.5 times slower than that of ouabain. Thus, the limited potency of ouabain 1,11,19-phosphate (**6**) as an inhibitor of the Na^+,K^+-ATPase (~2200-fold weaker than ouabain) is explained by the combination of slower binding and in particular the much faster dissociation rate (>200 times) relative to ouabain.

In other experiments (not shown), we investigated the possibility of "silent" binding by the 1,11,19-phosphate. In this hypothetical scenario, agents with silent effects might bind to regions within or overlapping the ouabain site on the Na^+,K^+-ATPase. Such agents might lack significant inhibitory effects but may compete effectively with the 1,5,19-phosphate or ouabain for binding. However, concentrations of the 1,11,19-phosphate (**6**) that were not themselves inhibitory did not affect the potency of the 1,5,19-phosphate (**5**). These results reveal that the 1,11,19-phosphate has no silent interactions with the Na^+,K^+-ATPase other than those that lead to inhibition of the enzyme.

^{3}H-Ouabain Binding Studies. Competition binding studies were performed to provide additional information on the mechanism of the inhibition of the Na^+,K^+-ATPase by ouabain 1,5,19- and 1,11,19-phosphate. Figure 7 shows the results of Scatchard analysis for the binding of ^{3}H-ouabain to the isolated Na^+,K^+-ATPase and the effect of the unlabeled phospho-ouabain analogues. The binding reaction was performed using K^+-free conditions in a 3 h incubation at 37 °C supported by Mg^{2+} and inorganic phosphate. Under these conditions, the binding of ^{3}H-ouabain was described by a single class of sites with an apparent dissociation constant of 3.9 nM and an maximum extrapolated binding density of 0.118 pmol. In the presence of 25 nM ouabain 1,5,19-phosphate or 500 nM ouabain 1,11,19-phosphate, the apparent dissociation constants for binding of ^{3}H-ouabain were reduced (21.6 and 6.4 nM, respectively) while the extrapolated maximal binding (0.117 and 0.115 pmol,

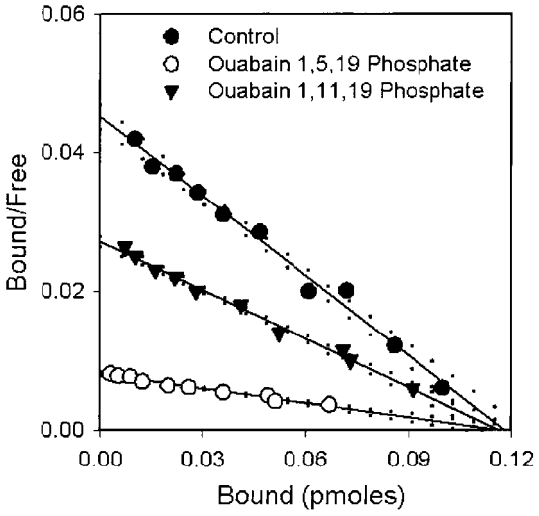

FIGURE 7: Effect of ouabain 1,5,19- and 1,11,19-phosphates on binding of ^{3}H-ouabain to Na^+,K^+-ATPase: Scatchard analysis. Dog kidney Na^+,K^+-ATPase was incubated for 3 h at 37 °C with ^{3}H-ouabain in the absence (●) or presence of 25 nM ouabain 1,5,19 phosphate (○) or 500 nM ouabain 1,11,19 phosphate (▼). Each point is the mean of triplicate determinations. The solid lines were fitted to the data by linear least squares regression. In each case the regression coefficients were >0.93. The dots adjacent to the regression lines are the 95th percentile confidence limits. See Materials and Methods for other details.

respectively) was similar to that using ^{3}H-ouabain alone. These results indicate that the macroscopic mechanism of inhibition of the Na^+,K^+-ATPase by both phospho-ouabain analogues is mediated via interactions with the ouabain binding site.

DISCUSSION

In the present studies, we used two stable conformationally locked analogues of ouabain to determine the significance of conformational flexibility in the steroid nucleus in the A ring region. Previous studies (*6*) showed that borate freely forms tetrahedral complexes with the 1,11,19- and 1,5,19-hydroxyl groups in ouabain that influence the conformation of the steroidal A-ring. However, these complexes were labile so that their specific interactions with the sodium pump could not be easily studied. Accordingly, similarities in the size and bond orientations of borate and phosphate led us to consider the latter as a means to generate stable covalent analogues of ouabain with different A-ring conformers.

We used an MDCK cell-based assay to evaluate the interaction between the sodium pump and the ouabain phosphates in a physiological environment. Ouabain at 10^{-5} M or higher concentrations appeared to saturate most of the sodium pumps on MDCK cells in our assay conditions, in which a subconfluent culture ($\sim 1-2 \times 10^5$ cells) was placed in each 3 μL assay chamber. As the number of sodium pumps on subconfluent MDCK cells has been shown to be $\sim 8 \times 10^7$ pumps per cell (*8*), the upper limit of pump concentration can be estimated at $\sim 10^{-5}$ M. It is, therefore, understandable that concentrations of ouabain $<10^{-6}$ M along with the relatively short exposure of the cells to this agent in a potassium-containing medium did not generate consistent cellular responses in our system. However, saturating concentrations of ouabain maximally decreased the extracellular acidification rate by 15−20%. This value is a little smaller than the reported fraction (ca. 25%) of cellular ATP consumed by the sodium pump in MDCK cells, which was estimated on the basis of the measurements of O_2 consumption and lactic acid production in suspension culture (*11*). In other renal epithelial cells and tissues, much larger values, i.e., up to 40% of cellular metabolic activity, have been attributed to the sodium pump (*2*). These differences might simply come from the differences in experimental methods and conditions. Another possible reason is the preferential coupling between glycolysis and the sodium pump in MDCK cells (*12*). If oxidative metabolism produces more acids for the synthesis of each ATP molecule than glycolysis in our experimental condition, the measurement of extracellular acidification rates could underestimate the fraction of cellular ATP metabolism mediated by the sodium pump.

Both the cell- and enzyme-based assays revealed that the two different A-ring conformations of native ouabain differ greatly in their biological potency. Ouabain 1,5,19-phosphate (**5**) largely retained the original inhibitory potency of ouabain whereas the activity of ouabain 1,11,19-phosphate (**6**) turned out to be much weaker in both assays. Although there are some important differences between the cell- and enzyme-based assays, the overall consistency of the two assays in terms of the primary conclusions reinforces the view that the pH microphysiometer can be used to monitor bulk sodium pump activity in living cells.

Studies with the isolated Na^+,K^+-ATPase showed that the phospho-ouabain analogues appeared to be purely competitive inhibitors of ^{3}H-ouabain binding. The high potency of ouabain 1,5,19-phosphate (**5**) in both the ATPase and binding assays indicates that the β-face of the ouabain molecule is not directly involved in an interaction with the cardenolide-binding site on the sodium pump. In other words, the 1,5,-19-OH groups in ouabain are most likely pointing toward the aqueous phase from inside or on the surface of the sodium pump. The decreased potency of ouabain 1,11,19-phosphate likely arises from the loss of favorable interactions with the sugar and cardenolide binding site(s) and/or the addition of unfavorable steric repulsions. One possible cause for this decreased activity is the deformation and limited flexation of the hydrophobic α-face of this analogue. While potent inhibitory activity of the 1,5,19-phosphate indicated that the β-face around the A/B-ring moiety is not directly involved in the interaction with the sodium pump, the role of the hydrophobic α-face has not been clarified. Many cardiac steroids have a "hydrophobic cavity" on their α-face thought to interact with one or more hydrophobic amino acid residues. In addition to the deformation of the α-face in ouabain 1,11,19-phosphate (**6**), the rhamnose is effectively placed on an "equatorial" 3β-O location that seems destined to lead to unfavorable steric repulsions and reduced interaction with other regions of the ouabain-binding site. This likely underlies the rapid dissociation of the 1,11,19 analogue.

Binding kinetics studies on ouabain and the 1,5,19-phosphate provided a novel insight into the molecular level interaction between ouabain and the sodium pump. Ouabain 1,5,19-phosphate binds to and dissociates from the isolated Na^+,K^+-ATPase somewhat faster than ouabain. The faster binding of the 1,5,19-phosphate (**5**) infers that ouabain has an A-ring chair conformation when it initially binds to the sodium pump. Conformational flexibility of the A-ring in

ouabain may therefore be expected to slow the binding of ouabain relative to its 1,5,19-phosphate. However, once the ouabain molecule becomes bound, the structural flexibility in the A-ring favoring the twist-boat conformation appears to enhance the lifetime of ouabain−Na^+,K^+-ATPase complexes. Thus, increased rigidity of the A-ring in **5** coupled with unimpeded flexibility in the BC-rings probably accounts for both the faster binding and dissociation relative to ouabain. When taken together, our results suggest that subtle flexibility of the steroid nucleus in ouabain is essential for the attainment of high-affinity binding. As the potency of ouabain is affected markedly by ligand type and concentration (*3*), it appears that the binding site in the sodium pump is structurally dynamic. This may explain why ouabain, whose structure permits some flection once bound, exhibits slower dissociation kinetics and higher overall potencies than many other structurally related cardiotonic steroid cardenolides.

Although the microphysiometry and enzyme assay results were mostly consistent, some differences were noted. One example is the dissociation rate profile of ouabain 1,5,19-phosphate. The 1,5,19-phosphate dissociated ∼16 times faster than ouabain from the purified Na^+,K^+-ATPase (Figure 5B), whereas the dissociation rate (recovery rate constant) of the 1,5,19-phosphate in the microphysiometry assay was only 3 times greater than that for ouabain (Figure 3B). As both assays gave comparable dissociation profiles in the case of ouabain, the discrepancy largely came from the 1,5,19-phosphate. Possible causes include the difference in the turnover rate of the sodium pump, differences in the ligand conditions in the cell and ATPase systems, and the fast association of the 1,5,19-phosphate. In particular, the latter may allow some of the dissociated 1,5,19-phosphate to rebind, and this could lead to an underestimate of the dissociation rate. Direct observation of the binding and dissociation of the phospho analogues was not feasible in the cell studies because our attempts to microsynthesize the analogues in radiolabeled form were not successful.

The overshoot of the acidification rate following the washout of ouabagenin is an interesting physiological phenomenon captured by the microphysiometer. Ouabagenin lacks the sugar moiety and dissociates from sodium pumps rapidly. When the sodium pump is inhibited to a significant extent, the large increase in intracellular sodium will fuel an overshoot in pump activity if the bound inhibitor can dissociate rapidly. The overshoot persists until the excess intracellular sodium has been pumped out and the pump rate returns to normal. Therefore, the recovery and value of the acidification rate following removal of ouabagenin is probably limited by cellular metabolic rates and thus may tend to underestimate the rate of dissociation of ouabagenin from the pump. No overshoot was found in the case of 10^{-4} M ouabain 1,11,19-phosphate although the compound appears to dissociate from the pump rapidly. This almost certainly reflects the lower potency of this analogue at the dose used so that the increase in intracellular sodium would have been less marked and insufficient to induce an overshoot.

The turnover rate of the purified Na^+,K^+-ATPase preparation from dog kidney is between 8000 and 10 000 min^{-1} (*25*), whereas the sodium pumps in MDCK cells have a rate between 4000 and 6000 min^{-1} (*11*). As ouabain preferentially binds to and stabilizes the E_2P form of the Na^+,K^+-ATPase, we wondered whether the slow-binding kinetics of ouabain could be specifically linked with the frequency of A-ring twist-boat to chair transitions and the rates at which E_2P forms and decays. On the basis of previously described NMR studies obtained at −20 °C in DMSO/$CDCl_3$ (*13*), peak splitting of the 1-C resonance (68.59 ppm/6859 Hz and 64.80 ppm/6480 Hz) in ouabain indicates that the A-ring changes its conformation <841 times/s. In water at physiological temperature, we predict the exchange rate of A-ring conformation to be greater than the estimated rate (841 times/s). We compared the frequency of the A-ring transitions with published first-order rate constants (*10*) for the relevant reaction cycle intermediates of the sodium pump assuming 37 °C, complete saturation, and a Q_{10} of 2.6 (*16*). Our calculations indicate that the deocclusion and release of three sodium ions from the phosphorylated form of the pump, E_1−P ($3Na^+$), that leads to formation of E_2P occurs ∼600 times s^{-1}. Once formed, the rapid binding and occlusion of potassium ions, i.e., $E_2P \rightarrow E_2(2K^+)$ occurs at ∼1300 s^{-1}. As expected, the lifetime of E_2P is short when extracellular potassium is fully saturating while at physiological concentrations of this ion, the rate of the $E_2P \rightarrow E_2(2K^+)$ reaction is likely to be 40−50% slower (i.e., 650−780 s^{-1}). This will lengthen the lifespan of E_2P and enhance the interaction probability with ouabain. Therefore, although exact values for the various parameters have not been measured, it is of interest that the rates of formation and decay of E_2P are of a similar magnitude to the frequency of the A-ring oscillations in ouabain. When taken together, the aforementioned calculations suggest that the distinct potencies of the two conformationally locked ouabain phosphates reveal an ability of ouabain to synchronize its conformation with a dynamic receptor. In particular, the conformational flexations of the A-ring appear to be especially important in facilitating the most favorable interactions with the sugar binding site once the steroid has bound.

While this paper was in revision, an article appeared by Middleton et al. (*14*) describing the use of a series of synthetic ouabain acetonide analogues to locate the cardenolide binding site in the Na^+,K^+-ATPase using solid-state NMR. The deduced orientation of those analogues is consistent with our conclusion regarding an aqueous orientation for the β-face of the steroid. Moreover, the NMR study showed that the sugar group in the acetonide analogues was highly mobile and not in meaningful contact with amino acid residues in the H1−H2 transmembrane region of the Na^+,K^+-ATPase. However, by analogy with the ouabain 1,11,19-phosphate we describe, the steroidal A-ring in the 1,19-acetonides may be conformationally locked. It is of interest that the ouabain 1,19-acetonides and the ouabain 1,11,19-phosphate were uniformly weak inhibitors of the Na^+,K^+-ATPase compared with ouabain, consistent with the proposal of suboptimal positioning and increased mobility of the sugar. While the latter probably accounts for the low potency of the acetonide derivatives as inhibitors of the Na^+,K^+-ATPase, the conclusion that the sugar remains mobile when ouabain is bound now appears uncertain. In this regard, the unique properties of the ouabain phosphates we describe may be of particular utility and relevance for further investigation of the topology of the ouabain-binding site.

In summary, we have synthesized and tested two novel conformationally locked phospho isomers of ouabain in

which selective tethering of the hydroxyls on the β-face of the steroid moiety led to unexpectedly large differences in biological activity. The results show that the high potency of ouabain as a sodium pump inhibitor is linked with flection of the steroid nucleus especially in the A-ring and that the ability to harmonize receptor and ligand dynamics is an important determinant of activity in this system.

ACKNOWLEDGMENT

We are grateful to Dr. Yasuhiro Itagaki (Columbia University) for the measurement of mass spectra and to Ms. Veronique Timmermans and Dr. Kelly J. Cassutt (Molecular Devices) for their help and instructions in the Cytosensor microphysiometer assay.

REFERENCES

1. Beck, M., Szalay, K. S., Nagy, G. M., Tóth, M., and de Châtel, R. (1996) *Endocrine Res. 22*, 845−849.
2. De Weer, P. (1992) in *The Kidney: Physiology and Pathophysiology* (Seldin, D. W., and Giebisch, G., Eds.) pp 93−112, Raven Press, New York.
3. Hamlyn, J. M., Harris, D. W., and Ludens, J. H. (1989) *J. Biol. Chem. 264*, 7395−7494.
4. Hamlyn, J. M., Hamilton, B. P., and Manunta, P. (1996) *J. Hypertens. 14*, 151−167.
5. Jorgensen, P. L. (1975) *Q. Rev. Biophys. 7*, 239−274.
6. Kawamura, A., Guo, J., Itagaki, Y., Bell, C., Wang, Y., Haupert, G. T., Jr., Magil, S., Gallagher, R. T., Berova, N., and Nakanishi, K. (1999) *Proc. Natl. Acad. Sci. U.S.A. 96*, 6654−6659.
7. Kawamura, A. (1999) Ph.D. Thesis, pp 132, Department of Chemistry, Columbia University, New York.
8. Kennedy, B. G., and Lever, J. E. (1984) *J. Cell. Physiol. 121*, 51−63.
9. Laredo, J., Hamilton, B. P., and Hamlyn, J. M. (1994) *Endocrinology 135*, 794−797.
10. Läuger, P., and Apell, H.-J. (1986) *Eur. Biophys. J. 13*, 309−321.
11. Lynch, R. M., and Balaban, R. S. (1987) *Am. J. Physiol. 252*, C225−C231.
12. Lynch, R. M., and Balaban, R. S. (1987) *Am. J. Physiol. 253*, C269−C276.
13. McIntyre, D. D., Germann, M. W., and Vogel, H. J. (1990) *Can. J. Chem. 68*, 1263−1270.
14. Middleton, D. A., Rankin, S., Esmann, M., and Watts, A. (2000) *Proc. Natl. Acad. Sci. U.S.A. 97*, 13602−13607.
15. Owicki, J. C., Bousse, L. J., Hafeman, D. G., Kirk, G. L., Olson, J., Wada, H. G., and Parce, J. W. (1994) *Annu. Rev. Biophys. Biomol. Struct. 23*, 87−113.
16. Post, R. L., Sen, A. K., and Rosenthal, A. S. (1965) *J. Biol. Chem. 240*, 1437−1444.
17. Schneider, R., Wray, V., Nimtz, M., Lehmann, W. D., Kirch, U., Antolovic, R., and Schoner, W. (1998) *J. Biol. Chem. 273*, 784−792.
18. Schoner, W., Ilberg, C., Kramer, R., and Seubert, W. (1967) *Eur. J. Biochem. 1*, 334−343.
19. Schönfeld, W., Weiland, J., Lindig, C., Masnyk, M., Kabat, M. M., Kurek, A., Wicha, J., and Repke, K. R. H. (1985) *Naunyn-Schmiedebergs Arch. Pharmacol. 329*, 414−426.
20. Stimers, J. R., Shigeto, N., and Lieberman, M. (1990) *J. Gen. Physiol. 95*, 61−76.
21. Suschitzky, J. L., and Wells, E. (1990) in *Comprehensive Medicinal Chemistry* (Hansch, C., Ed.) Pergamon Press, Oxford.
22. Yoda, A., Yoda, S., and Sarrif, A. M. (1973) *Mol. Pharmacol. 9*, 766−773.
23. Yoda, A. (1973) *Mol. Pharmacol. 9*, 51−60.
24. Yoda, A. (1974) *Ann. N.Y. Acad. Sci. 242*, 598−616.
25. Yoda, A., and Yoda, S. (1977) *Mol. Pharmacol. 13*, 352−361.

BI0101751